TSINGHUA SCIENCE AND TECHNOLOGY
ISSN 1007-0214 06/24 pp368–385
DOI: 10.26599/TST.2023.9010067
Volume 29, Number 2, April 2024

A Constraint Adaptive Multi-Tasking Differential Evolution Algorithm: Designed for Dispatch of Integrated Energy System in Coal Mine

Canyun Dai, Xiaoyan Sun*, Hejuan Hu, Yong Zhang, and Dunwei Gong

Abstract: The dispatch of integrated energy systems in coal mines (IES-CM) with mine-associated supplies is vital for efficient energy utilization and carbon emissions reduction. However, IES-CM dispatch is highly challenging due to its feature as multi-objective and strong multi-constraint. Existing constrained multi-objective evolutionary algorithms often fall into locally feasible domains with poorly distributed Pareto front, which greatly deteriorates dispatch performance. To tackle this problem, we transform the traditional dispatch model of IES-CM into two tasks: the main task with all constraints and the helper task with constraint adaptive. Then we propose a constraint adaptive multi-tasking differential evolution algorithm (CA-MTDE) to optimize these two tasks effectively. The helper task with constraint adaptive is developed to obtain infeasible solutions near the feasible domain. The purpose of this infeasible solution is to transfer guiding knowledge to help the main task move away from local search. Additionally, a dynamic dual-learning strategy using DE/current-to-rand/1 and DE/current-to-best/1 is developed to maintain task diversity and convergence. Finally, we comprehensively evaluate the performance of CA-MTDE by applying it to a coal mine in Shanxi Province, considering two IES-CM scenarios. Results demonstrate the feasibility of CA-MTDE and its ability to generate a Pareto front with exceptional convergence, diversity, and distribution.

Key words: dispatch; integrated energy system; coal mine; evolutionary multi-tasking; constraint; differential evolution

1 Introduction

The integrated energy system (IES) has gained popularity in recent years due to the rapid development of Internet technology and renewable energy. IES aims to coordinate the production, conversion, and consumption of multiple energy sources, such as electricity, heat, and cooling. This structure revolutionizes the traditional energy usage scenario, where different energy infrastructures typically operate separately[1]. As a result, IES is a more effective approach to improving energy efficiency, promoting the utilization of renewable energy, and reducing environmental pollution compared to traditional paradigms.

The dispatch of IES has a significant impact on promising the system safety, economy, and environment protection. Among the existing IES, the dispatch of integrated energy systems in coal mines (IES-CM) is of utmost importance due to its high energy consumption and high emissions. For this purpose, Hu et al.[2] first proposed a coal mine integrated energy system and established a multi-objective dispatch model with objectives as economic operation cost, carbon transaction cost, and degree of consumer dissatisfaction. Moreover, the traditional solver CPLEX is used to solve the problem. Huang et al.[3] constructed a two-stage robust stochastic dispatch model in the coal mine integrated energy system and used the robust

• Canyun Dai, Xiaoyan Sun, Hejuan Hu, and Yong Zhang are with School of Information and Control Engineering, China University of Mining and Technology, Xuzhou 221116, China. E-mail: TB21060011B4@cumt.edu.cn; xysun78@126.com; 1101481742@qq.com; yongzh401@126.com.
• Dunwei Gong is with School of Information Science and Technology, Qingdao University of Science and Technology, Qingdao 266061, China. E-mail: dwgong@vip.163.com.
* To whom correspondence should be addressed.
Manuscript received: 2023-04-26; revised: 2023-06-10; accepted: 2023-06-26

stochastic optimization method to solve it. Wang et al.[4] developed a multi-scenario operation model for IES-CM and suggested an autonomous intelligence to effectively solve it.

The IES-CM dispatch is a new type of multi-constrained and multi-objective optimization problem. This is because the problem involves a large number of constraints, including equality ones such as electrical, cooling, and heat balance constraints, and inequality constraints such as device capacity constraints, operation constraints, and ramp rate constraints. These constraints make the problem highly coupled and temporally dependent. Currently, some multi-objective evolutionary algorithms (MOEAs) have been developed for the IES dispatch in different scenarios. For example, Wang et al.[5] used the non-dominated sorting genetic algorithm II (NSGA-II) to optimize the model of electro-thermal IES. Wu et al.[6] presented an improved multi-objective multifactorial evolutionary algorithm to address multi-objective dispatch of IES considering biogas-solar-wind renewables. Qiao et al.[7] proposed an ε-constraint fruit fly optimization algorithm to solve the IES multi-objective model considering installation configurations. Dong et al.[8] developed a constrained multi-objective state transition algorithm to solve the IES planning model containing uncertainty. Compared with traditional solvers (such as CPLEX and Gurobi) or mathematical programming methods, the MOEAs can obtain a set of non-dominated solutions for decision makers to choose. However, due to the lack of efficient constraint handling method, the diversity, convergence, and uniformity of Pareto front (PF) generated are insufficient.

The development of constrained MOEAs (CMOEAs) provides an effective way to deal with constrained problems. Representative outcomes include multi-population based[9–11] and multi-stage based ones[12, 13]. In the last two years, a new type of CMOEAs with evolutionary multi-tasking (EMT)[14] method is developed for constrained multi-objective problems (CMOPs). The EMT proposed by Gupta et al.[14] in 2015 is a new research paradigm, and its feasibility and effectiveness have been verified in various real-world problems[15–17]. Based on the EMT method, Qiao et al.[18] suggested a novel EMT-based constrained multi-objective optimization framework. This framework assigns two populations to optimize these two tasks in parallel. This is the first study to use EMT to solve CMOPs. Later, Qiao et al.[19] proposed a new multi-tasking constrained multi-objective optimization framework, in which a dynamic auxiliary task is created to assist in solving the CMOPs (the main tasks). Ming et al.[20] developed a tritask framework with constrained dominance principle (CDP) based, Pareto dominance based, and constraint relaxation based tasks, and designed a new algorithm. Compared with methods based on multi-population and multi-stage, the EMT-based methods have great attraction and novelty in dealing with constraints. However, these corresponding studies have not been extended to serve the IES dispatch problems.

Motivated by the above observation and analysis, we here develop a constraint adaptive multi-tasking differential evolution algorithm (CA-MTDE) to handle strong coupling and timing constraints in the multi-constraint and multi-objective IES-CM dispatch problem. First, a multi-objective dispatch model for the IES-CM that aims to minimize the cost on system operation and abandoned energy is introduced. Second, the CA-MTDE using a helper task with constraint adaptive (HT-CA) under the multi-tasking framework to help the main task (original problem) find the feasible optimal PF is proposed. Additionally, a dynamic dual-learning (DDL) mutation strategy is developed based on two well-known differential evolution (DE) operators, DE/current-to-rand/1 and DE/current-to-best/1[21], to balance the diversity and convergence of the two tasks at different stages of evolution. DE proposed by storn and price[22], as a simple yet powerful method, is chosen because of its successful application in a large number of optimization problems[23, 24]. Finally, the proposed algorithm is verified using an example of a coal mine located in Shanxi. The results indicate that the proposed CA-MTDE algorithm outperforms CPLEX and six representative CMOEAs in terms of obtaining the best extreme and compromise solutions. The algorithm also achieves optimal values for two performance indicators, inverted generation distance (IGD) and hypervolume (HV). Furthermore, the Wilcoxon signed ranks test is conducted for IGD and HV in both scenarios to demonstrate the significant superiority of the proposed algorithm. The major contributions of this paper are highlighted as follows:

(1) Propose a CA-MTDE for IES-CM dispatch problem

To handle the strong coupling and timing constraints in IES-CM, this paper transforms the multi-constraint and multi-objective IES-CM dispatch problem into a multi-tasking optimization problem by using the idea of

EMT. Therefore, a CA-MTDE is proposed.

(2) Design an HT-CA for the proposed CA-MTDE

In CA-MTDE, a helper task with constraint adaptive known as HT-CA is developed to assist the main task in discovering globally viable PF. The HT-CA dynamically adjusts the constraint boundaries of the helper task based on the number of iterations. This feature enables the HT-CA to continuously generate possible infeasible solutions near feasible domains throughout evolution, providing diversified evolutionary paths for the main task through knowledge transfer.

(3) Develop a DDL strategy for the proposed CA-MTDE

In CA-MTDE, a DDL strategy is further developed to effectively balance the diversity and convergence of the two tasks at different evolutionary stages. Specifically, the DDL strategy combines the DE/current-to-rand/1 and DE/current-to-best/1 operators to dynamically update individuals to learn search characteristics from different individuals. The performance of the two mutation operators shows that the DDL strategy can not only promote the diversity by learning from randomly selected population individuals but also accelerate convergence by utilizing information from optimal individuals in the population.

(4) Verify effectiveness and competitiveness of CA-MTDE on actual IES-CM

Two system scenarios are carried out with the integrated energy system of a coal mine in Shanxi Province as an example. The optimization results show that our CA-MTDE algorithm is competitive in acquiring a PF with a good distribution and broad diversity in two scenarios, when compared with the CPLEX solver and six representative CMOEAs.

The paper is organized as follows. Section 2 introduces the multi-objective dispatch model for IES-CM and provides a detailed description of the model development. Section 3 addresses the proposed CA-MTDE for solving the IES-CM model, including a thorough explanation of the methodology. Section 4 demonstrates the results of our experimental study, including statistical analysis and visual explanations. Finally, in Section 5, we summarize our findings, discuss their implications, and outline directions for future research.

2 Multi-Objective Dispatch Model for IES-CM

2.1 IES-CM description

A schematic representation of an IES-CM structure is depicted in Fig. 1. It comprises four key components: energy supply, energy conversion, energy storage, and energy demand. The energy supply component consists of three sub-components: energy market, renewable energy sources, and coal mine-associated energy. The energy market sub-component primarily encompasses grid supply and gas supply. Renewable energy sources include photovoltaic (PV) and wind turbines (WT). Coal mine-associated energy comprises ventilation air methane (Vam), air heat, mine water, and geothermal energy. The energy conversion component incorporates various units such as combined heating and power

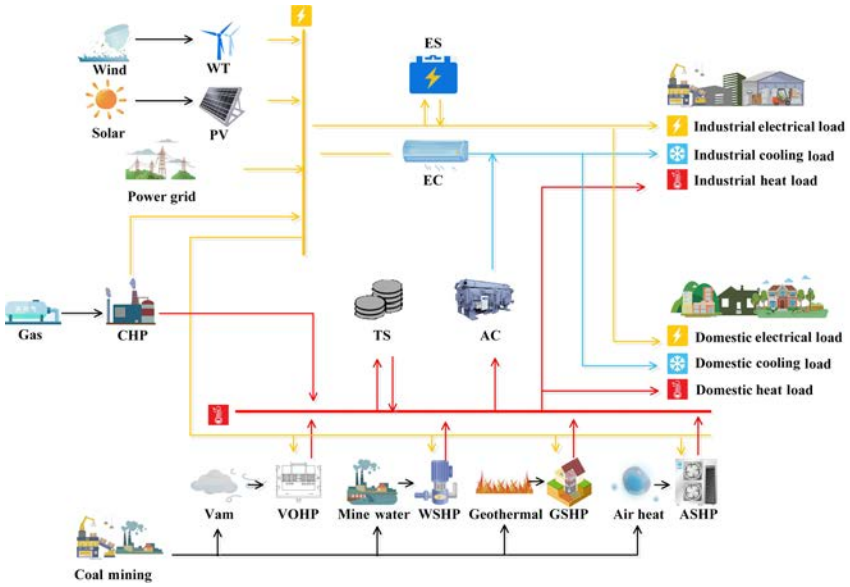

Fig. 1 Structure of the IES-CM.

(CHP), Vam oxidation heat pumps (VOHP), water source heat pumps (WSHP), ground source heat pumps (GSHP), air source heat pumps (ASHP), absorption chillers (AC), and electric chillers (EC). Energy storage encompasses electric storage (ES) and heat storage (HS). Finally, the energy demand component includes electrical load, cooling load, and heat load for industrial and domestic purposes.

The IES-CM has unique features that distinguish it from general IESs. Firstly, the associated energy generated in the coal mine production process is fully converted into heat energy, thereby avoiding energy wastage and reducing environmental pollution. Secondly, the associated energy exhibits strong coupling properties, as it serves as both a consumer of electrical energy and a supplier of thermal energy. Thirdly, the energy demand in IES-CM has distinct characteristics, encompassing flexible loads required by the domestic sector and rigid loads required by the coal mine production process. Consequently, the study of the IES-CM dispatch problem and the development of effective solving algorithms hold significant practical significance.

2.2 IES-CM dispatch model

In this section, we construct a two-objective day-ahead dispatch model that comprehensively considers various operational constraints. The acronyms and notations used here are listed in Table 1.

2.2.1 Optimization objectives

Objective 1: The daily comprehensive operational cost (OC) of the IES-CM[2] is expressed below, which includes the energy purchase cost (PC) and the cost of equipment operation and maintenance (OM):

$$\text{MinOC} = \text{PC} + \text{OM} \tag{1}$$

$$\text{PC} = \sum_{t=1}^{T} (c_t^{\text{grid}} \times E_t^{\text{grid}} + c_t^{\text{gas}} \times Q_t^{\text{CHP}}) \tag{2}$$

$$\text{OM} = \sum_{t=1}^{T} \sum_{k=1}^{N} c_k^{\text{maint}} \times E_t^k \tag{3}$$

where $T = 24$ is the total number of time periods; N represents the total number of devices; E_t^{grid} and c_t^{grid} are the electricity provided by grid and the price of electricity at time t, respectively; Q_t^{CHP} and c_t^{gas} mean natural gas consumption and gas price at time t, respectively; c_k^{maint} denotes the operating and maintenance cost factor of the k device; and E_t^k indicates energy output of the k device at time t. The devices considered in this paper include WT, PV, CHP, VOHP, WSHP, EC, and AC.

Objective 2: The abandoned energy cost (AE) objective is defined as follows, which comprises the cost of abandoning renewable energy and coal mine-associated energy.

$$\text{AE} = \sum_{t=1}^{T} \sum_{k=1}^{N} c_k^{\text{abandon}} \times (E_{t,\max}^k - E_t^k) \tag{4}$$

where c_k^{abandon} represents the penalty factor for abandoning energy of the k device; and $E_{t,\max}^k$ is the maximum output of the k device. Related devices include WT, PV, VOHP, and WSHP.

2.2.2 Constraint

In ensuring the safety of a system, it is important to satisfy the operational constraints. These constraints include inequality ones that limit the acceptable operating range for each device and equality constraints that describe the balance between supply and demand.

Energy balance constraints. In the electro-thermal IES-CM, energy balance constraints include electricity, heat, and cooling balances between energy supply and demand.

(1) Electric balance constraint

$$E_t^{\text{grid}} + E_t^{\text{PV}} + E_t^{\text{WT}} + E_t^{\text{CHP}} = E_t^{\text{load}} + E_t^{\text{VOHP}} + E_t^{\text{WSHP}} + E_t^{\text{EC}} \tag{5}$$

where E_t^{load} represents the electric load of the system at time t.

(2) Heat balance constraint

$$H_t^{\text{CHP}} + H_t^{\text{VOHP}} + H_t^{\text{WSHP}} = H_t^{\text{load}} + H_t^{\text{AC}} \tag{6}$$

where H_t^{load} represents the heat load of the system at time t.

(3) Cooling balance constraint

$$Q_t^{\text{EC}} + Q_t^{\text{AC}} = Q_t^{\text{load}} \tag{7}$$

where Q_t^{load} represents the cooling load of the system at time t.

Energy conversion constraints. The energy conversion constraints are expressed as follows:

$$H_t^{\text{CHP}} = \eta_{\text{CHP}}^{\text{e2h}} \times E_t^{\text{CHP}} \tag{8}$$

$$H_t^{\text{VOHP}} = \eta^{\text{VOHP}} \times E_t^{\text{VOHP}} \tag{9}$$

$$H_t^{\text{WSHP}} = \eta^{\text{WSHP}} \times E_t^{\text{WSHP}} \tag{10}$$

$$Q_t^{\text{EC}} = \eta^{\text{EC}} \times E_t^{\text{EC}} \tag{11}$$

$$Q_t^{\text{AC}} = \eta^{\text{AC}} \times E_t^{\text{AC}} \tag{12}$$

where $\eta_{\text{CHP}}^{\text{e2h}}$ represents the thermoelectric ratio; η^{VOHP} and η^{WSHP} represent the conversion efficiency of VOHP and WSHP from electricity to heat, respectively; η^{EC} is the conversion efficiency of EC from electricity to

Table 1 Nomenclature.

Acronym/ notation	Description	Acronym/ notation	Description
AC	Absorption chiller	η^{WSHP}	Energy efficiency coefficient of WSHP
AE	Abandoned energy cost	$\eta_{\mathrm{CHP}}^{\mathrm{e2h}}$	Thermoelectric ratio of CHP
AR-MOEA	IGD-NS based MOEA with reference point adaptation	μ_i	Satisfaction degree of the i-th optimal solution
c-DPEA	Dual-population based evolutionary algorithm	$\sigma(0)$	Initial constraint violation value
C-NSGA-II	Constrained NSGA-II	c_k^{abandon}	Penalty factor for abandoning energy of the k device
C-NSGA-III	Constrained NSGA-III	c_k^{maint}	Operating and maintenance cost factor of the k device
CCMO	Coevolutionary constrained multi-objective optimization	c_t^{grid}, c_t^{gas}	Electricity price and gas price at time t
CDP	Constraint dominance principle	D	Index representing population dimension
CHP	Combined heating and power	$E_{t,\min}^{\mathrm{grid}}$, $E_{t,\max}^{\mathrm{grid}}$	Minimum and maximum output powers of the grid at time t
CMOEAs	Constrained multi-objective evolutionary algorithms	$E_{t,\min}^{k}$, $E_{t,\max}^{k}$	Lower and upper limits of the output powers of the k device at time t
CMOPs	Constrained multi-objective optimization problems	E_t^k, H_t^k, Q_t^k	Electric, heat, and cooling outputs of the k device at time t
DE	Differential evolution	E_t^{load}, H_t^{load}, Q_t^{load}	Electric, heat, and cooling loads of the system at time t
EC	Electric chiller	F	Mutation factor
EMT	Evolutionary multitasking	$f_m^{\max}$, $f_m^{\min}$	Maximum and minimum function values of the m-th objective
IES	Integrated energy system	$f_{i,m}$	The m-th objective function value of the i-th individual
IES-CM	Integrated energy system in coal mine	g, G	Current and maximum iterations
MOEAs	Multi-objective evolutionary algorithms	k, N	Index representing device
MSCMO	Multi-stage constrained multi-objective evolutionary algorithms	M	Number of objective functions
OC	Operational cost	Nt	Number of the PF point
OM	Equipment operational and maintenance cost	Off_i	Offspring population
PC	Energy purchase cost	Pop_i, $\mathrm{Pop}_{\mathrm{best}}$	The i-th individual and best individual of the current population
PF	Pareto front	$R_{\mathrm{low}}^{\mathrm{CHP}}$, $R_{\mathrm{up}}^{\mathrm{CHP}}$	Ramp rate lower and up limit of the CHP unit at time t
PV	Photovoltaic	t, T	Index representing time period
VOHP	Vam oxidation heat pump	$V(x)$	Total constraint violation value for x
WSHP	Water source heat pump		
WT	Wind turbine		
η^{AC}	Energy efficiency coefficient of AC		
η^{EC}	Energy efficiency coefficient of EC		
η^{VOHP}	Energy efficiency coefficient of VOHP		

cooling; and η^{AC} represents the conversion efficiency of AC from heat to cooling.

Device operation constraints. The power output range of each device must be kept within the maximum and minimum limits to ensure the safety and reliability of the system. This is because the characteristics of the device play a crucial role in determining the constraints of its operation.

$$E_{t,\min}^{k} \leqslant E_t^k \leqslant E_{t,\max}^{k} \tag{13}$$

where $E_{t,\min}^{k}$ and $E_{t,\max}^{k}$ are the lower and upper limits of the output power of the k device, respectively, including PV, WT, CHP, VOHP, WSHP, EC, and AC.

Grid operational constraints. The electricity purchasing from the power grid should satisfy the following grid operational constraints:

$$E_{t,\min}^{\mathrm{grid}} \leqslant E_t^{\mathrm{grid}} \leqslant E_{t,\max}^{\mathrm{grid}} \tag{14}$$

where $E_{t,\min}^{\mathrm{grid}}$ and $E_{t,\max}^{\mathrm{grid}}$ are the minimum and maximum power of the grid, respectively.

CHP ramp rate constraint. The CHP is a highly efficient way of generating heat and electricity simultaneously. The system uses natural gas to produce both forms of energy, but it is important to ensure that the power output of each generator does not vary too much. This is because excessive stresses on the boiler and combustion equipment can occur if the change rate of power output is too high. Therefore, it is necessary to impose a ramp rate constraint to avoid drastic power variations of CHP between adjacent timeslots.

$$E_t^{\mathrm{CHP}} - E_{t-1}^{\mathrm{CHP}} \leqslant R_{\mathrm{up}}^{\mathrm{CHP}} \tag{15}$$

$$E_{t-1}^{\mathrm{CHP}} - E_t^{\mathrm{CHP}} \leqslant R_{\mathrm{low}}^{\mathrm{CHP}} \tag{16}$$

where $R_{\mathrm{low}}^{\mathrm{CHP}}$ and $R_{\mathrm{up}}^{\mathrm{CHP}}$ are the ramp down and ramp up limits of the CHP unit, respectively.

2.3 Pareto optimization formulation

The aforementioned dispatch of IES-CM can be formulated as a constrained multi-objective Pareto optimization problem as follows:

$$\begin{cases} \min F(x) = (\mathrm{OC}(x), \mathrm{AE}(x)); \\ x = [E_t^{\mathrm{grid}}, e_t^{\mathrm{PV}}, E_t^{\mathrm{WT}}, e_t^{\mathrm{CHP}}, H_t^{\mathrm{VOHP}}, \\ \quad H_t^{\mathrm{WSHP}}, Q_t^{\mathrm{EC}}, Q_t^{\mathrm{AC}}]; \\ \text{s.t., energy balance constraints, Eqs. (5)–(7);} \\ \quad \text{energy conversion constraints, Eqs. (8)–(12);} \\ \quad \text{device operation constraint, Formula (13);} \\ \quad \text{grid operational constraint, Formula (14);} \\ \quad \text{CHP ramp rate constraints, Formulas (15)} \\ \quad \text{and (16)} \end{cases} \tag{17}$$

where x represents a variable to be optimized of the IES-CM problem and time $t = 1, 2, \ldots, 24$.

Discussion: our problem vs. constrained multi-objective benchmark functions. In essence, the IES-CM dispatch problem is a constrained multi-objective problem. However, unlike the constrained multi-objective benchmark functions proposed so far, our problem has practical physical significance. There are three specific differences as follows. (1) Dynamic characteristic: In our problem, the optimization variables change in each hour, i.e., depending on time t. So our problem can be thought of as dynamic. (2) Strong coupling characteristic of decision space: From the expression of Eq. (17), the number of constraints is greatly more than the number of objectives, besides, it is clear that our constraints strongly separate the decision space in many sub-spaces, which is in sharp contrast to the benchmark function in limiting the target space. In addition, as shown in Eqs. (5)–(12), variables are represented linearly by equality constraints. Compared with the existing benchmark functions, the strong coupling of decision space further increases the difficulty in solving the problem. (3) Timing characteristic: Under the influence of ramp rate constraint, the optimization variables related to CHP will be further restricted by the up and down time, resulting in a greatly reduced search domain of the variable (as shown in Formulas (15) and (16)). However, timing characteristics are not reflected in the current benchmark functions. Therefore, a more effective algorithm in dealing with both multiple objectives and strong constraints must be developed to fit these characteristics of this kind of problem.

3 Proposed CA-MTDE for Solving IES-CM Dispatch Problem

In this section, we propose a CA-MTDE to effectively optimize the IES-CM dispatch. Equation (17) is first reformulated into two tasks, i.e., a main task as Eq. (17) and an HT-CA. The HT-CA is developed here to powerfully handle strong coupling and timing constraints. The main idea of HT-CA gradually reduces the constraint boundaries according to the evolutionary generations of DE, and some infeasible solutions nearest to the adjusted feasible domain are explored. These solutions will be used in the knowledge sharing of CA-MTDE to maintain a high correlation between the main and helper tasks. With HT-CA, the evolutionary paths of the main task can be well guided to escape from the local optimum search. Moreover, to maintain the balance of diversity and convergence between the two tasks during different search stages, a dynamic dual-learning (DDL) mutation strategy is designed. The DE/current-to-rand/1 or DE/current-to-best/1 is dynamically selected in the entire evolution process to generate offspring individuals, which learns the search performance of different DE operators in the distinctive tasks. In the early stage, this maintains the diversity of the population to explore more feasible domains, while in the late stage, it improves the convergence to locate the optimal solution. Furthermore, we introduce an environment selection mechanism integrating multiple constraint handling techniques and a compromise solution selection strategy with fuzzy decision into the proposed algorithm. This ensures that the algorithm can handle various constraints effectively and select the best solution that balances the trade-off between different objectives. Figure 2 plots the framework of the proposed CA-MTDE.

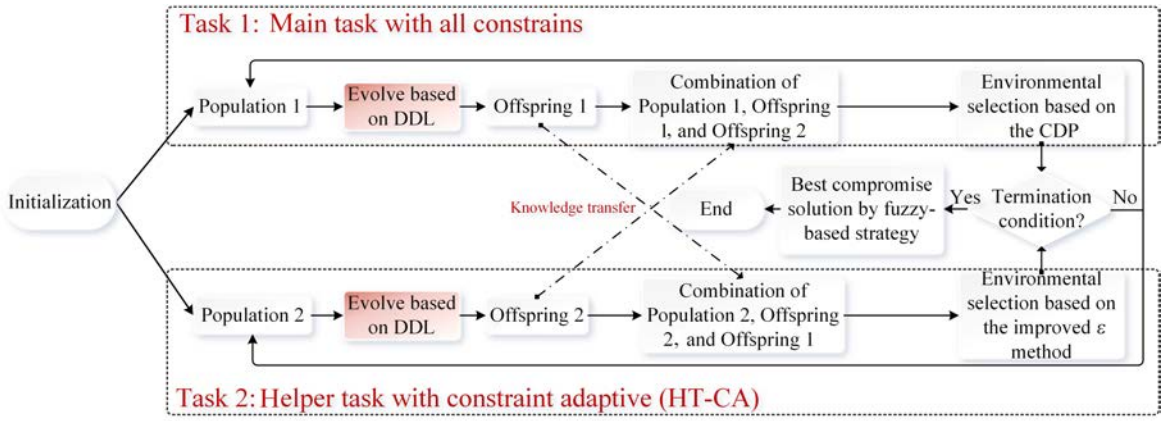

Fig. 2 Framework of the proposed CA-MTDE.

3.1 A novel helper task with constraint adaptive

In this section, the helper task with constraint adaptive is created to help solve the main task with all constraints. HT-CA adaptively reduces the constraint boundary during evolution, resulting in some infeasible solutions close to multiple feasible domains. Such infeasible solutions then are transferred to the main task through individual-based knowledge transfer[19], which helps the main task escape from the locally feasible domain. The formulation of HT-CA can be described as follows:

$$\min F(x) = (\mathrm{OC}(x),\ \mathrm{AE}(x)), \text{s.t.}, V(x) \leqslant \sigma_g \quad (18)$$

$$\sigma_g = \sigma(0) \cdot \mathrm{e}^{(\mathrm{tt} \cdot g/G)} \quad (19)$$

where g and G are the current and maximal generations, respectively; $V(x)$ is the total constraint violation value for x; $\sigma(0)$ is the initial constraint violation value which equals to the maximal V value of both initial main population and helper population; and tt is the parameter that controls the rate of descent of σ_g and is set to -12.

Discussion: Equations (18) and (19) show that the two tasks have the same objective. However, unlike the main task, the constraint boundary $\sigma(g)$ of the helper task gradually decreases with the number of iterations. Therefore, auxiliary tasks can not only explore some infeasible solutions close to the feasible domain in the evolutionary but also gradually push the population into the feasible domain by constraining dynamic changes. Overall, the two tasks have different evolutionary trajectories that can provide useful information to each other via knowledge transfer.

3.2 Dynamic dual-learning mutation strategy

The DDL mutation strategy is developed to balance the diversity and convergence of the two tasks in the entire evolution. It combines two DE operators with different search characteristics, namely DE/current-to-rand/1 and DE/current-to-best/1, and designs a dynamic parameter. In DE/current-to-rand/1, each target vector learns from a randomly selected individual, thus promoting the diversity. By making use of the information of the best individual, DE/current-to-best/1 can speed up the convergence. Additionally, a parameter decreasing with the number of iterations is designed to dynamically select one of the two operators to produce the offspring. In the early stage, two tasks select the DE/current-to-rand/1 with greater probability to increase the population diversity and explore more feasible domains. In the late stage, two tasks select the DE/current-to-best/1 to improve the convergence and find the optimal solution. The formulation of the DDL mutation strategy is as follows:

$$\mathrm{Off}_i = \begin{cases} \mathrm{Pop}_i + \mathrm{rand} \cdot (\mathrm{Pop}_{r_1} - \mathrm{Pop}_i) + \\ \quad F \cdot (\mathrm{Pop}_{r_2} - \mathrm{Pop}_{r_3}),\ \text{if rand} < d_g; \\ \mathrm{Pop}_i + F \cdot (\mathrm{Pop}_{\mathrm{best}} - \mathrm{Pop}_i) + \\ \quad F \cdot (\mathrm{Pop}_{r_1} - \mathrm{Pop}_{r_2}),\ \text{otherwise} \end{cases} \quad (20)$$

$$d_g = (1 - g/G)^{D/20} \quad (21)$$

where Pop_i and $\mathrm{Pop}_{\mathrm{best}}$ are the i-th individual and best individual of the current population, respectively; r_1, r_2, and r_3 are mutually distinct target vectors randomly selected from the population; and F is randomly selected from a scaling factor pool $\{0.6, 0.8, 1.0\}$. The reasons for the above random parameters setting are that they are simple and their effectiveness has been validated in Ref. [25]. "rand" is a uniformly distributed random number between 0 and 1; and D is the population dimension. It can be noted from Eq. (21) that the parameter d_g dynamically reduces from 1 to 0 as the number of iterations increases.

3.3 Environment selection mechanism

In a multi-tasking framework, the environment selection mechanism plays a significant role in determining the algorithm's performance[26, 27]. In this paper, we adopt several powerful constraint handling strategies to assist different task evolution in achieving efficient search. The CDP[28] and the improved ε constraint method[29, 30] are the most classical and efficient constraint handling mechanisms. However, they pay different attention to the objective and constraint. The CDP has an inherent preference for constraints, thus attracting a population towards the feasible region promptly. In contrast, the improved ε constraint method tends to focus on the objective, using the information on infeasible solutions to guide the population search. Therefore, for the two tasks constructed in this paper, the main task chooses the CDP method to quickly locate multiple feasible regions, and the helper task uses the improved ε constraint method to balance the conflict between the objective and constraint.

3.4 Fuzzy-based decision-making strategy

An optimal compromise solution must be selected after the PF of IES-CM dispatch is obtained. However, accurately describing the judgment of decision-makers is difficult. Accordingly, a fuzzy-based decision-making strategy[31] is used here to recommend a promising solution to the decision-maker by taking full account of the fuzziness of human decision-making. To be specific, the satisfaction degree of each Pareto optimal solution is calculated using the formula as follows:

$$\mu_i = \frac{\sum_{m=1}^{M} \mu_{im}}{\sum_{i=1}^{\mathrm{Nt}} \sum_{m=1}^{M} \mu_{im}} \tag{22}$$

$$\mu_{im} = \begin{cases} 1, & \text{if } f_{im} \leqslant f_m^{\min}; \\ \frac{f_m^{\max} - f_{im}}{f_m^{\max} - f_m^{\min}}, & \text{if } f_m^{\min} \leqslant f_{im} \leqslant f_m^{\max}; \\ 0, & \text{if } f_{im} \geqslant f_m^{\max} \end{cases} \tag{23}$$

where M denotes the number of objective functions ($M = 2$ in this paper); Nt is the number of the PF point; f_{im} is the m-th objective function value of the i-th PF point; and $f_m^{\max}$ and $f_m^{\min}$ are maximum and minimum of the m-th objective, respectively. The solution with the greatest satisfaction will be selected as the best compromise solution.

3.5 Pseudo-code of CA-MTDE

The pseudo-code of CA-MTDE is presented in Algorithm 1. Initially, two populations with N individuals are randomly initialized in the search space and evaluated under the corresponding task. The main loop begins with updating $\sigma(g)$ according to HT-CA. Then, each population uses the DDL mutation strategy to generate the offspring population, which is then evaluated. Additionally, two offspring populations are merged with the main task and helper task populations, respectively, to complete the knowledge transfer. Finally, the environment selection mechanism described in Section 3.3 is used to generate new populations, and the best compromise solution is obtained by a fuzzy-based strategy.

Algorithm 1 Pseudo-code of CA-MTDE

Input: N: size of the population, D: dimension of the population, G: maximum number of iterations, u_x: upper limit of problem, and l_x: lower limit of problem
Output: Op: feasible Pareto optimal solutions

```
% Initialization Pop_1 and Pop_2
Pop_1 ← Randomly generate N individuals
Pop_2 ← Randomly generate N individuals
% Evaluate individuals
Evaluate Pop_1 on the main task
Evaluate Pop_2 on the helper task
% The main loop
for g = 1 : G do
    % Update σ(g)
    σ_g = σ(0) · e^(−12·g/G)
    % Generate offspring based on DDL mutation strategy
    Update dynamic threshold d_g = (1 − g/G)^(D/20)
    if rand < d_g then
        Off_1 ← Use DE/current/to/rand/1 operator to generate offspring based on the Pop_1
        Off_2 ← Use DE/current/to/rand/1 operator to generate offspring based on the Pop_2
    else
        Off_1 ← Use DE/current/to/best/1 operator to generate offspring based on the Pop_1
        Off_2 ← Use DE/current/to/best/1 operator to generate offspring based on the Pop_2
    end if
    % Evaluate new individuals
    Evaluate Off_1 on the main task
    Evaluate Off_2 on the helper task
    % Knowledge transfer for different tasks
    Pop_1 ← Pop_1 ⋃ Off_1 ⋃ Off_2
    Pop_2 ← Pop_2 ⋃ Off_2 ⋃ Off_1
    % Environmental selection
    Pop_1 ← Select N solutions from Pop_1 by the CDP method
    Pop_2 ← Select N solutions from Pop_2 by the improved ε method
    % Elite solution selection
    Op ← The best compromise solution by fuzzy-based strategy in Pop_1
end for
Output the optimal dispatch result
```

4 Application and Analysis

To demonstrate the effectiveness of our proposed algorithm in solving the IES-CM dispatch problem, we have applied our algorithm to a typical IES-CM in Shanxi Province, China, by considering two dispatch scenarios, i.e., electricity-heat and electricity-heat-cooling. Shanxi Province, located in the northwest of China, experiences higher heat demand during winter, which makes the dispatch more complex and challenging. Accordingly, we here experimentally demonstrate the dispatch results of the IES-CM on a randomly selected day during winter. Our experiments and analysis will focus on the following aspects:

(1) The performance of our proposed CA-MTDE algorithm with that of the CPLEX solver is compared to demonstrate the feasibility of our approach in solving the IES-CM dispatch.

(2) The distribution, diversity, and convergence of our algorithm are evaluated by comparing it with six popular and representative CMOEAs. Additionally, the quantitative metrics to measure the multi-objective optimization performance are presented.

(3) The real energy dispatch of the selected solutions obtained using our CA-MTDE algorithm with the decision-making strategy is illustrated, which intuitively exhibits the results of the optimized objectives on operation and energy abandon costs. These results will be addressed in detail in the following subsections.

4.1 Problem scenarios and parameter settings

In this paper, two different dispatch scenarios are considered to verify the feasibility and effectiveness of the proposed algorithm in solving IES-CM problems of different difficulties. The differences between the two scenarios are described below:

Scenario 1: Electric-heat IES-CM including 6×24 decision variables and 10×24 constraints.

Scenario 2: Electric-heat-cooling IES-CM including 8×24 decision variables and 13×24 constraints.

The parameter settings include system parameters and algorithm parameters. The system parameters are set as follows. Each energy load demand, wind, and solar forecast data of the coal mine[2] are shown in Fig. 3. Figure 4 provides the electricity price and gas price. Thereinto, the real-time electricity price for power purchase is adopted, while the gas price is fixed at 0.2 RMB/kW · h. Moreover, Table 2 provides the related parameters, mainly including

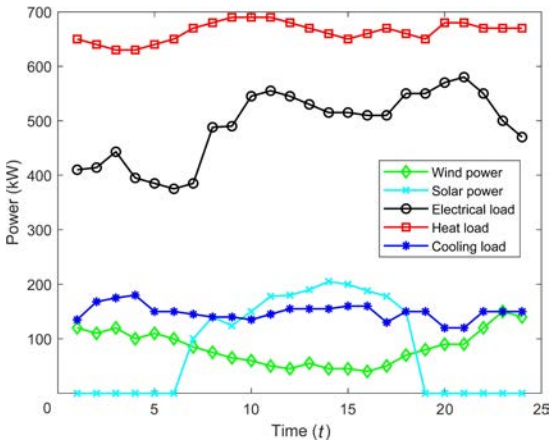

Fig. 3 Wind power, solar power, electrical load, heat load, and cooling load curves in IES-CM.

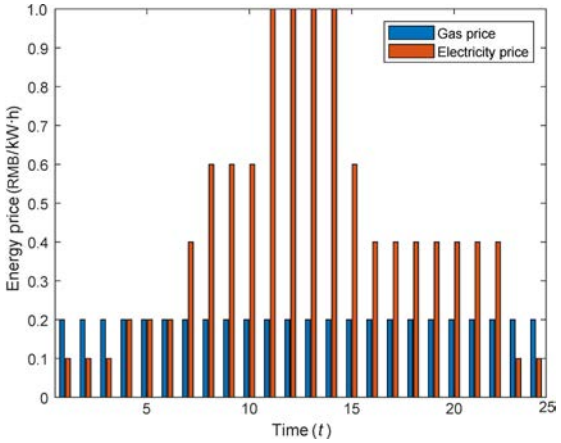

Fig. 4 Energy purchase price of each period.

device technical and economic parameters. The system parameters of the two scenarios are consistent. The algorithm parameters are given below. The population size is set to 100, and the maximal number of function evaluations is set to 300 000. Comparison of algorithms contain constraint NSGA-II (C-NSGA-II)[32], constraint NSGA-III (C-NSGA-III)[33], IGD-NS-based MOEA with reference point adaptation (AR-MOEA)[34], co-evolutionary CMOEA (CCMO)[9], multi-stage CMOEA (MSCMO)[12], and dual-population-based evolutionary algorithm (c-DPEA)[10]. All methods apply these settings for a fair comparison. The parameter settings of all the compared algorithms are the same as suggested in their corresponding original papers. Each algorithm runs independently 20 times on each scenario to ensure reliability. We use the PlatEMO platform[35] to carry out a series of simulation experiments on a personal computer with an Intel (R) Core i7-11700 2.5 GHz CPU and 16.00 GB of RAM.

Table 2 Device technical and economic parameters.

Device	Parameter	Value
PV	Operational and maintenance cost (RMB/kW · h)	$c_{\mathrm{PV}}^{\mathrm{maint}}$ =0.3
	Abandoned energy cost (RMB/kW · h)	$c_{\mathrm{PV}}^{\mathrm{abandon}}$ =0.8
	Minimum output (kW)	$E_{\mathrm{min}}^{\mathrm{PV}}$ =0
	Maximum output (kW)	$E_{\mathrm{max}}^{\mathrm{PV}}$ =predicted value
WT	Operational and maintenance cost (RMB/kW · h)	$c_{\mathrm{WT}}^{\mathrm{maint}}$ =0.25
	Abandoned energy cost (RMB/kW · h)	$c_{\mathrm{WT}}^{\mathrm{abandon}}$ =0.6
	Minimum output (kW)	$E_{\mathrm{min}}^{\mathrm{WT}}$ =0
	Maximum output (kW)	$E_{\mathrm{max}}^{\mathrm{WT}}$ =predicted value
CHP	Operational and maintenance cost (RMB/kW · h)	$c_{\mathrm{CHP}}^{\mathrm{maint}}$ =0.1
	Minimum output (kW)	$E_{\mathrm{min}}^{\mathrm{CHP}}$ =0
	Maximum output (kW)	$E_{\mathrm{max}}^{\mathrm{CHP}}$ =300
	Ramp down (kW)	$R_{\mathrm{low}}^{\mathrm{CHP}}$ =50
	ramp up (kW)	$R_{\mathrm{up}}^{\mathrm{CHP}}$ = −50
	Efficiency of gas to electricity of CHP	$\eta_{\mathrm{CHP}}^{\mathrm{e}}$ =0.4
	Thermoelectric ratio of CHP	$\eta_{\mathrm{CHP}}^{\mathrm{e2h}}$ =1.25
VOHP	Operational and maintenance cost (RMB/kW · h)	$c_{\mathrm{VOHP}}^{\mathrm{maint}}$ =0.55
	Abandoned energy cost (RMB/kW · h)	$c_{\mathrm{VOHP}}^{\mathrm{abandon}}$ =0.7
	Minimum output (kW)	$E_{\mathrm{min}}^{\mathrm{VOHP}}$ =10
	Maximum output (kW)	$E_{\mathrm{max}}^{\mathrm{VOHP}}$ =150
	Conversion efficiency of VOHP	η^{VOHP} =3.3
WSHP	Operational and maintenance cost (RMB/kW · h)	$c_{\mathrm{WSHP}}^{\mathrm{maint}}$ =0.6
	Abandoned energy cost (RMB/kW · h)	$c_{\mathrm{WSHP}}^{\mathrm{abandon}}$ =0.75
	Minimum output (kW)	$E_{\mathrm{min}}^{\mathrm{WSHP}}$ =10
	Maximum output (kW)	$E_{\mathrm{max}}^{\mathrm{WSHP}}$ =120
	Conversion efficiency of WSHP	η^{WSHP} =3.5
Grid	Minimum output (kW)	$M_{\mathrm{low}}^{\mathrm{grid}}$ =0
	Maximum output (kW)	$M_{\mathrm{up}}^{\mathrm{grid}}$ =800
EC	Operational and maintenance cost (RMB/kW · h)	$c_{\mathrm{EC}}^{\mathrm{maint}}$ =0.2
	Minimum output (kW)	$E_{\mathrm{min}}^{\mathrm{EC}}$ =0
	Maximum output (kW)	$E_{\mathrm{max}}^{\mathrm{EC}}$ = 280
	Conversion efficiency of EC	η^{EC} =0.65
AC	Operational and maintenance cost (RMB/kW · h)	$c_{\mathrm{AC}}^{\mathrm{maint}}$ =0.3
	Minimum output (kW)	$E_{\mathrm{min}}^{\mathrm{AC}}$ =0
	Maximum output (kW)	$E_{\mathrm{max}}^{\mathrm{AC}}$ =260
	Conversion efficiency of AC	η^{AC} =0.7

4.2 Feasibility of CA-MTDE: Comparing with CPLEX

The feasibility of the proposed CA-MTDE is first verified by comparing its performance with that of the CPLEX solver. We here select the CPLEX as a basis for comparison because it is one of the most popular and successful methods for solving IES dispatch[36]. Additionally, a global optimum can be guaranteed with CPLEX for a single-objective dispatch. For multi-objective dispatch, a weighted sum is often used to convert it into a single object to fit CPLEX. If the solution obtained using our algorithm is no worse than that of CPLEX with the same weight setting, then it is rational to conclude that our CA-MTDE algorithm is feasible in solving the CM-IES dispatch problem.

The solution with the weight of (0.5, 0.5) for the two objectives in CPLEX is selected to compare with the compromise solution of the proposed algorithm. Figure 5 shows the best PF obtained by CA-MTDE in 20 independent runs. In Fig. 5, the endpoints of the PF marked with pink diamond symbols are the extremal objective values, and their corresponding solutions are called extremal solutions. The green square represents the solution of CPLEX at the weight of (0.5, 0.5). The compromised solution selected with the fuzzy-based method is marked with a red star.

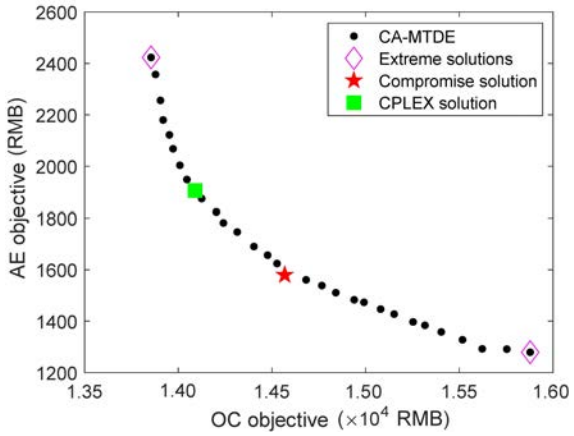

(a) Comparison for Scenario 1

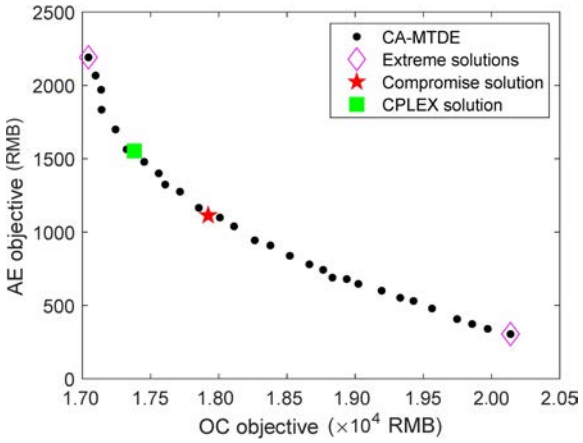

(b) Comparison for Scenario 2

Fig. 5 Comparison of CA-MTDE and CPLEX in two scenarios.

From Fig. 5, the solutions obtained by CPLEX in two scenarios are (OC=14 090.00 RMB and AE=1905.40 RMB) and (OC=17 381.00 RMB and AE=1552.80 RMB), respectively. While the compromised solutions obtained by CA-MTDE in two scenarios are (OC=14 568.20 RMB and AE= 1579.59 RMB) and (OC=17 922.50 RMB and AE=1113.52 RMB), respectively. By comparing the above results, it can be found that the solutions obtained by CPLEX and CA-MTDE are non-dominated by each other, which shows the feasibility of our method. More importantly, extremal solutions of our method in a single run, i.e., OC=13 854.60 RMB and AE=1279.09 RMB for Scenario 1, and OC=17 044.70 RMB and AE=304.58 RMB for Scenario 2, indicate that it is more superior than CPLEX solutions. These insights show that our proposed method is not only feasible but also more competitive in a single run.

4.3 Performance of CA-MTDE in convergence, diversity, and distribution: Comparing with six competitors

In this section, the performance and effectiveness of the proposed CA-MTDE in solving the IES-CM problem are investigated by experimental study in the two scenarios and comparison with six representative CMOEAs. First, two commonly used metrics, i.e., IGD[37] and HV[38], are adopted to evaluate the convergence, diversity, and distribution of the competing methods. Second, the PF results covering the extreme solutions and compromised solutions of all the algorithms are further demonstrated and compared to validate the efficiency of CA-MTDE.

The IGD focuses on measuring how close the obtained PF is to the real optimal one, reflecting the convergence of the algorithm. A smaller IGD value indicates better convergence. It is worth noting that the reference sets of all comparison algorithms for calculating IGD metrics are the same. Tables 3 and 4 show the comparison results among seven different algorithms for two scenarios in terms of IGD, including the best IGD, worst IGD, median IGD, average IGD, and standard deviation (Std) obtained in 20 independent runs. The best values are marked in bold.

From Tables 3 and 4, the following observations can be made. **For Scenario 1:** (1) The proposed CA-MTDE achieves the optimal values for the best IGD, the worst IGD, the median IGD, and the average IGD. These

Table 3 Statistical results of the IGD for Scenario 1.

Approach	IGD				
	Best	Worst	Median	Average	Std
C-NSGA-II[32]	260.4955	463.5850	351.7192	353.1253	51.0919
C-NSGA-III[33]	424.9600	721.3459	624.2890	587.0626	109.3484
AR-MOEA[34]	295.3867	611.8954	445.9509	457.0581	89.3221
CCMO[9]	295.5503	721.9138	474.5953	484.1106	128.8969
MSCMO[12]	250.1973	580.4449	353.2276	385.1867	102.3591
c-DPEA[10]	347.0088	773.0050	466.9761	494.6345	122.7260
CA-MTDE	**8.6495**	**21.4439**	**12.4785**	**12.3608**	**2.7359**

Table 4 Statistical results of the IGD for Scenario 2.

Approach	IGD				
	Best	Worst	Median	Average	Std
C-NSGA-II[32]	882.7935	1980.7900	1421.4216	1358.1275	325.0488
C-NSGA-III[33]	903.2327	1767.4543	1076.4971	1160.7775	246.4176
AR-MOEA[34]	735.5289	1886.219	1200.6720	1266.4509	360.1127
CCMO[9]	950.3119	1968.3491	1385.7196	1367.5746	306.1954
MSCMO[12]	661.9584	2148.7422	1417.5973	1331.4550	411.2590
c-DPEA[10]	634.6970	2143.2812	1312.5246	1396.1636	428.8972
CA-MTDE	**626.8547**	**797.4544**	**746.7169**	**736.2671**	**53.4987**

values are 1/30, 1/27, 1/28, and 1/29 of the corresponding sub-optimal algorithms MSCMO, MSCMO, C-NSGA-II, and C-NSGA-II, respectively. (2) Move eyes on the Std values, the proposed algorithm has the minimum one as 2.7359, which is about 1/25 of that of C-NSGA-II, the second better algorithm. **For Scenario 2:** (1) Our method improves by 5%, 55%, 31%, and 37% compared to the suboptimal algorithms c-DPEA, C-NSGA-III, C-NSGA-III, and C-NSGA-III in the best IGD, worst IGD, median IGD, and average IGD, respectively. (2) The proposed algorithm has the minimum Std value of 53.4987, which is about 1/5 of that of the second better algorithm C-NSGA-III. (3) Comparing the IGD values in Scenario 1, it is evident that the IGD value of our method in Scenario 2 is much larger than that in Scenario 1, because Scenario 2 is more complex, which increases the difficulty of algorithm optimization. However, CA-MTDE obtains the optimal values in both scenarios, indicating that the distance between true PF points achieved by the proposed algorithm and the optimal solutions is relatively closer. Moreover, our algorithm has higher robustness and stability than the other algorithms in the two scenarios, which is greatly beneficial to solving practical IES dispatch. According to the above analysis, it is rational to conclude that the proposed algorithm achieves an outperformed PF with the best convergence, robustness, and efficiency than other popular CMOEAs.

The HV reflects the diversity and distribution of the algorithm by calculating the volume enclosed by the solutions found by the algorithm and reference point. A smaller HV value indicates better diversity and distribution. Tables 5 and 6 list the HV results among seven different algorithms under two scenarios. **For Scenario 1:** (1) The best HV value of CA-MTDE is 1.0092, which is 16% higher than the second-ranked algorithm MSCMO. (2) The worst HV value of CA-MTDE is 0.9897, which is 36% higher than the second-ranked algorithm C-NSGA-II. (3) The median and average HV values of CA-MTDE are the best among all algorithms, which are 21% and 22% higher than the second-ranked algorithm C-NSGA-II. (4) The minimum Std value of the proposed algorithm is 0.0062, which is 94% lower than the second-ranked algorithm C-NSGA-II. **For Scenario 2:** (1) The best, the worst, and the average HV values of CA-MTDE are 0.8530, 0.7868, and 0.8118, respectively, which are 4%, 47%, and 24% higher than the second-ranked algorithm MSCMO. (2) The median HV value of CA-MTDE is 24% higher than the second-ranked algorithm C-NSGA-III. (3) Observing the Std values, the minimum one of CA-MTDE is 0.0214, which is 73% lower than the second-ranked algorithm C-NSGA-III. (4) Similar to the IGD value, the HV value of our method in Scenario 2 is worse than that in Scenario 1 due to the increased difficulty of the problem. Nevertheless, our approach still achieves the best HV metric in Scenario 2. The Std results in the two scenarios show that our approach can operate in a more secure manner, which is critical to IES dispatch. Based on the above analysis, it can be easily concluded that the proposed algorithm has better diversity and distribution for solving the IES-CM.

Table 5 Statistical results of the HV for Scenario 1.

Approach	HV				
	Best	Worst	Median	Average	Std
C-NSGA-II[32]	0.8114	0.7300	0.7839	0.7808	0.0220
C-NSGA-III[33]	0.7306	0.5831	0.6590	0.6634	0.0513
AR-MOEA[34]	0.7859	0.6472	0.7273	0.7221	0.0378
CCMO[9]	0.7788	0.6157	0.7245	0.7147	0.0528
MSCMO[12]	0.8417	0.6704	0.7806	0.7683	0.0456
c-DPEA[10]	0.7262	0.5651	0.6911	0.6784	0.0463
CA-MTDE	**1.0092**	**0.9897**	**0.9980**	**0.9993**	**0.0062**

Table 6 Statistical results of the HV for Scenario 2.

Approach	HV				
	Best	Worst	Median	Average	Std
C-NSGA-II[32]	0.6962	0.3920	0.5409	0.5468	0.0902
C-NSGA-III[33]	0.7714	0.4139	0.6131	0.6105	0.0822
AR-MOEA[34]	0.7895	0.3464	0.5696	0.5713	0.1220
CCMO[9]	0.7153	0.4063	0.5146	0.5314	0.1050
MSCMO[12]	0.8136	0.4185	0.5823	0.6181	0.1323
c-DPEA[10]	0.7467	0.3289	0.5001	0.4942	0.1192
CA-MTDE	**0.8530**	**0.7868**	**0.8058**	**0.8118**	**0.0214**

To demonstrate the significant differences between the proposed algorithm CA-MTDE and its equivalents, we conduct a Wilcoxon signed ranks test[39] for IGD and HV metrics on two scenarios, with a significance level of 0.05. The results of the Wilcoxon signed ranks test are presented in Table 7. All p-values are less than 0.05, indicating a significant difference between CA-MTDE and each of the compared algorithms. In conclusion, the proposed CA-MTDE is more suitable for solving the IES-CM problem than the other comparison algorithms.

Table 8 displays the statistical results of extreme solutions obtained by all methods for Scenario 1. The elaborate discussion and analysis are provided below. **(1) Objective 1: OC objective.** The proposed CA-MTDE

Table 7 Wilcoxon signed ranks test of IGD and HV metrics under two scenarios.

CA-MTDE vs.	*p*-value			
	Scenario 1		Scenario 2	
	IGD	HV	IGD	HV
C-NSGA-II[32]	0.00	0.00	0.00	0.00
C-NSGA-III[33]	0.00	0.00	0.00	0.00
AR-MOEA[34]	0.00	0.00	0.00	0.00
CCMO[9]	0.00	0.00	0.00	0.00
MSCMO[12]	0.00	0.00	0.00	0.00
c-DPEA[10]	0.00	0.00	0.00	0.00

obtains the optimal extreme solution of 13 854.60 RMB. The OC value of C-NSGA-II is second only to that of CA-MTDE, with a difference of 166.07 RMB. The OC value of c-DPEA is the worst, and the difference in OC value between c-DPEA and CA-MTDE is 191.58 RMB. **(2) Objective 2: AE objective.** The proposed CA-MTDE acquires the optimal value of the AE objective, which is 1279.09 RMB. The AE value of MSCMO is slightly worse than the proposed algorithm, while c-DPEA performs the worst AE value among all the comparison algorithms, with 590.49 RMB more abandoned energy cost than the proposed CA-MTDE. In conclusion, our algorithm obtains optimal extremal solutions for both objectives in Scenario 1, showing a wider PF distribution obtained by CA-MTDE.

Table 9 presents the statistical results of extreme solutions obtained by seven methods for Scenario 2. The analysis is as follows. **(1) Objective 1: OC objective.** The OC values obtained by CA-MTDE are compared with those obtained by C-NSGA-II, C-NSGA-III, AR-MOEA, CCMO, MSCMO, and c-DPEA. The difference between the OC values is as follows: C-NSGA-II: 192.03 RMB, C-NSGA-III: 663.31 RMB, AR-MOEA: 910.66 RMB, CCMO: 1134.58 RMB, MSCMO: 1562.56 RMB, and c-DPEA: 1033.33 RMB. This result shows the competitiveness of the proposed algorithm in the OC objective. **(2) Objective 2: AE objective.** The proposed algorithm obtains the optimal value of 304.58 RMB for the AE objective. MSCMO is 665.86 RMB which is second only to our method, while c-DPEA with 1466.86 RMB is the worst performer. Overall, our approach achieves optimal extremal solutions for the OC and AE objectives in Scenario 2. The above analysis of the extreme solutions in the two scenarios concludes that our method can jump out of the locally feasible domain and obtain more diverse PF.

Tables 8 and 9 also present the optimal compromise solutions obtained by all algorithms through the fuzzy-based decision method. Further, to compare the compromised solutions of different algorithms, the average satisfactory degree (ASD)[40] is calculated. The bold values indicate the best results obtained. Based on the ASD value, the proposed CA-MTDE attains the best ASD value among seven algorithms (0.692 for Scenario 1 and 0.843 for Scenario 2). In other words, our method provides the best compromise solutions

Table 8 Extreme solutions and compromised solution obtained by different methods for Scenario 1.

Approach	OC objective		AE objective		Compromised solution		ASD
	OC (RMB)	AE (RMB)	OC (RMB)	AE (RMB)	OC (RMB)	AE (RMB)	
C-NSGA-II[32]	14 020.67	2298.24	14 628.88	1675.18	14 207.62	1883.32	0.679
C-NSGA-III[33]	14 023.53	2265.02	14 324.65	1832.36	14 111.29	1983.75	0.679
AR-MOEA[34]	14 035.20	2271.24	14 324.43	1836.49	14 125.99	1989.04	0.667
CCMO[9]	14 038.14	2284.72	14 370.81	1824.96	14 123.58	2000.65	0.680
MSCMO[12]	14 021.42	2267.62	14 626.06	1665.80	14 181.08	1909.21	0.665
c-DPEA[10]	14 046.18	2242.61	14 297.08	1869.58	14 143.92	1965.38	0.676
CA-MTDE	**13 854.60**	2423.26	15 878.37	**1279.09**	14 568.15	1579.59	**0.692**

Table 9 Extreme solutions and compromised solution obtained by different methods for Scenario 2.

Approach	OC objective		AE objective		Compromised solution		ASD
	OC (RMB)	AE (RMB)	OC (RMB)	AE (RMB)	OC (RMB)	AE (RMB)	
C-NSGA-II[32]	17 236.76	2095.48	17 804.46	1362.14	17 588.58	1401.84	0.663
C-NSGA-III[33]	17 708.04	1902.46	18 088.19	1229.08	17 765.50	1414.06	0.787
AR-MOEA[34]	17 955.39	2093.76	18 474.09	1335.39	18 044.71	1622.56	0.724
CCMO[9]	18 179.31	1849.01	18 548.47	1415.30	18 282.95	1488.61	0.775
MSCMO[12]	18 607.29	880.89	19 205.77	665.86	18 970.27	713.15	0.586
c-DPEA[10]	18 078.06	1779.19	18 525.37	1466.86	18 310.93	1484.64	0.754
CA-MTDE	**17 044.73**	2191.18	20 139.31	**304.58**	17 922.50	1113.52	**0.843**

for Scenario 1 (OC = 14 568.15 RMB and AE = 1579.59 RMB) and Scenario 2 (OC=17 922.50 RMB and AE= 1113.52 RMB). These results indicate that our method can provide more rational dispatch results for decision-makers.

Figure 6 presents the distribution of the PF achieved by our algorithm and the comparison algorithms in two different scenarios. Figure 6 clearly illustrates that the comparison algorithm performs better in Scenario 1 compared to Scenario 2. This difference may be attributed to the increased difficulty of the model in Scenario 2, which results in a narrower global feasible domain and an increased likelihood of the algorithm converging to local optima. However, our algorithm obtains an extensive and well-distributed PF in both scenarios. The comprehensive evaluation of various metrics, including IGD, HV, extreme solutions, compromised solutions, and PF distribution, across the two scenarios demonstrates that CA-MTDE outperforms the other six CMOEAs in terms of convergence, diversity, and distribution. Consequently, our algorithm proves to be more efficient in solving the IES-CM dispatch problem. In conclusion, the comparative analysis of CMOEAs for the IES-CM dispatch problem reveals that our algorithm outperforms other comparison algorithms in terms of convergence, diversity, and distribution. This study provides a valuable contribution to the field of the IES-CM dispatch problem.

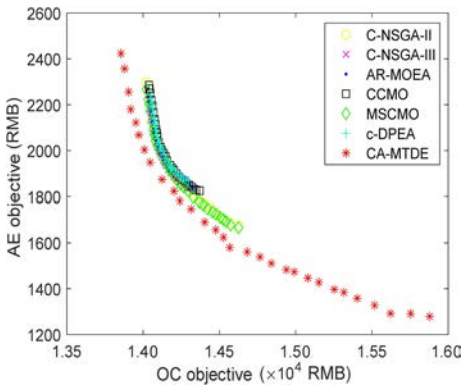

(a) PF of all algorithms for Scenario 1

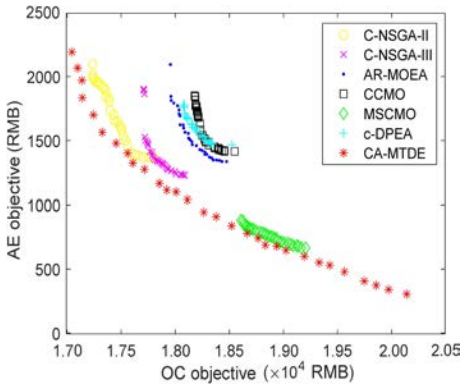

(b) PF of all algorithms for Scenario 2

Fig. 6 PF of all algorithms in two scenarios.

4.4 Real energy analysis: Compromised solutions for two IES-CM scenarios

To further demonstrate the feasibility and effectiveness of our algorithm in solving practical IES-CM dispatch, the energy input/output of each device in the two IES-CM scenarios is analyzed by selecting the compromised solutions of the two systems. The dispatch results of 24 h are shown in Figs. 7 and 8. The following will analyze the output of each device in each period from the supply end and demand end of multiple energy sources to explain the rationality and balance of the output of each device.

(1) Scenario 1: Electricity and heat balance analysis

Figure 7a illustrates the input/output results of electricity of each device. The electric input includes grid power (Egrid), CHP (Echp), WT (Ewt), and PV

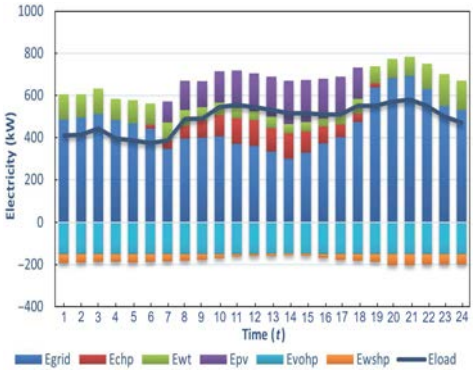

(a) Electricity input/output

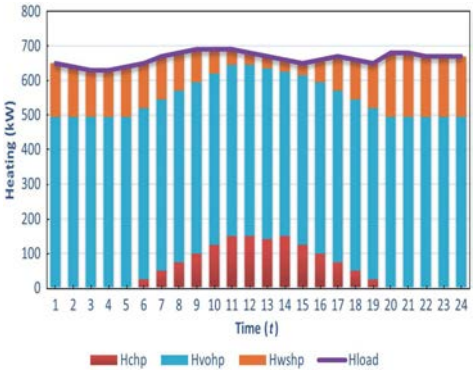

(b) Heat input/output

Fig. 7 Electricity and heat input/output of CA-MTDE for Scenario 1.

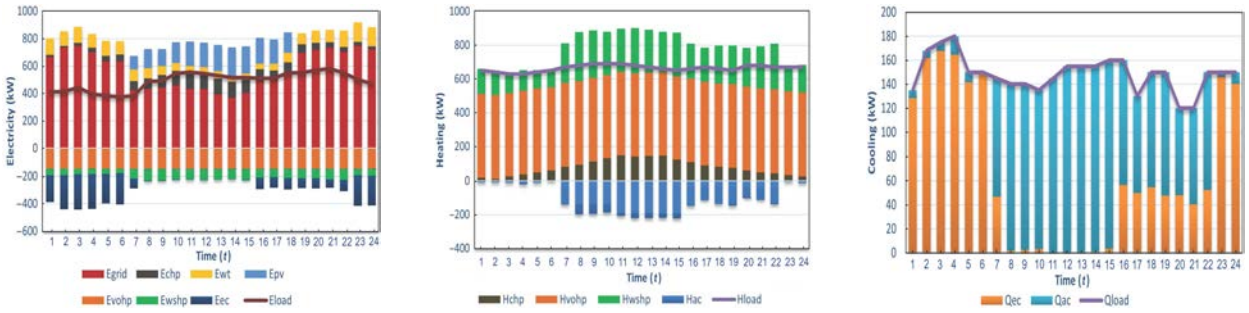

(a) Electricity input/output (b) Heat input/output (c) Cooling input/output

Fig. 8 Electricity, heat, and cooling input/output of CA-MTDE for Scenario 2.

(Epv). The electric output includes not only the electrical load (Eload) but also the electricity required by the electrothermic coupled conversion device VOHP and WSHP (Evohp and Ewshp). Several conclusions can be drawn from Fig. 7a. (1) During the 1–6 t and 18–24 t dispatch periods, the Egrid output is high, while in other periods, the Egrid output is less. This is reasonable because it is affected by the real-time electricity price shown in Fig. 4. (2) The outputs of Ewt and Epv are almost as high as predicted, indicating that renewable energy is fully utilized. (3) The energy input is equal to the output, indicating that the electricity balance constraint is satisfied.

The heat input mainly consists of three electrothermic coupled devices: CHP, VOHP, and WSHP (Hchp, Hvohp, and Hwshp), while the heat output only is the heat load (Hload). Several observations can be deduced from Fig. 7b. (1) The Hchp output is consistent with that of Echp in each period because the CHP is affected by the characteristic of fixing heat based on electricity. (2) The output of Hvohp reaches the maximum output in each period. This can be attributed to two reasons. Firstly, the VOHP has lower operation and maintenance costs, which means greater output can save economic costs. Secondly, the larger output of VOHP can make full use of the Vam generated in the coal mine production process to reduce energy waste and protect the environment. (3) The heat balance constraint is satisfied, so the output of Hwshp is affected by Hchp and Hvohp.

(2) Scenario 2: Electricity, heat, and cooling balance analysis

Figure 8a shows that the electricity input in Scenario 2 is consistent with that in Scenario 1, while the electricity output includes not only Eload, Evohp, and Ewshp but also Eec to meet the cooling load. From Fig. 8a, we can draw several conclusions. (1) During the period of 7–17 t, Egrid purchased from the grid decreases due to the rise in electricity prices. (2) When electricity prices peak, the output of Echp is increased to compensate for the lack of Egrid. (3) Ewt and Epv reach the maximum output of electricity because they aim to make full use of renewable energy sources. (4) The output sum of Egrid, Echp, Ewt, and Epv is equal to the Eload, indicating that the electrical balance is met. (5) The output characteristics of Egrid, Echp, Ewt, and Epv are similar to those of Scenario 1. However, the Qec output in Scenario 2 will increase the power demand and thus increase the power output. Therefore, the objective value of OC will increase compared to Scenario 1.

Figure 8b illustrates the input/output results of heat of each device. The heat input includes Hchp, Hvohp, and Hwshp, while the heat output contains not only the required heat load (Hload) but also the heat energy required by AC (Hac). The analysis is as follows. (1) Hvohp operates at maximum power due to lower operating costs and greater penalty costs. (2) During the period of 7–22 t, the output of Hwshp is higher to meet the cold demand of Hac. (3) The output of Hchp in each period is affected by the electricity price, and the output changes from less to more to less. (4) Heat balance is satisfied. (5) The output characteristics of Hvohp and Hwshp are similar to those of Scenario 1. Qac output further utilizes the associated energy generated in the coal mine production process, thereby reducing energy waste, so the AE objective is correspondingly reduced in Scenario 2.

Figure 8c is the input/output results of cooling of each device. The cooling load (Qload) has two sources: Qac and Qec. The heat for Qac comes from Vam and underground wastewater, while Qec uses electric energy from renewable sources. Some conclusions can be observed from Fig. 8c. (1) Qec provides most of the cooling load during periods 1–6 t and 23–24 t due to low electricity prices. (2) Qac provides most of the cooling

load during the 7–22 t period to reduce economic costs. (3) The cold balance is satisfied.

5 Conclusion

A new algorithm CA-MTDE is proposed to optimize the dispatch of IES-CM. This algorithm effectively addresses the multi-objective nature and strong multi-constraints of the problem by leveraging the concept of EMT. The proposed CA-MTDE optimizes two tasks: the main task with all constraints and the helper task with adaptive constraint. The HT-CA in CA-MTDE adaptively decreases constraint boundaries to preserve infeasible solutions near the feasible domain and employs knowledge transfer to continuously explore potentially feasible domains for the main task. This approach addresses strong coupling and timing constraints with efficiency. To balance population diversity and convergence of the two tasks, a DDL strategy is designed based on DE/current-to-rand/1 and DE/current-to-best/1. The DDL maximizes the potential of different individuals to search for characteristics. The effectiveness of our proposed algorithm is demonstrated by considering two dispatch scenarios based on a typical IES-CM in Shanxi Province, China. The comparison with CPLEX shows the feasibility of our approach in solving the IES-CM dispatch. Additionally, compared with six CMOEAs in terms of the IGD, HV, extreme solutions, and compromised solutions, our algorithm achieves better convergence, diversity, and distribution. Furthermore, we illustrate the real energy dispatch based on the compromised solutions obtained by CA-MTDE to intuitively showcase the energy output results of each device.

However, when the IES-CM model incorporates more devices, the complexity of solving the model will increase, potentially affecting the feasibility and effectiveness of our proposed method. Therefore, for future research, we plan to develop a new multi-tasking framework and design a knowledge transfer strategy that integrates domain knowledge to address the dispatch problem of large-scale and strongly constrained IES-CM systems.

Acknowledgment

This work was supported by the National Key R&D Program of China (No. 2021YFE0199000) and the National Natural Science Foundation of China (No. 62133015).

References

[1] J. Xu, Y. Chen, J. Wang, P. D. Lund, and D. Wang, Ideal scheme selection of an integrated conventional and renewable energy system combining multi-objective optimization and matching performance analysis, *Energy Convers. Manag.*, vol. 251, p. 114989, 2022.

[2] H. Hu, X. Sun, B. Zeng, D. Gong, and Y. Zhang, Enhanced evolutionary multi-objective optimization-based dispatch of coal mine integrated energy system with flexible load, *Appl. Energy*, vol. 307, p. 118130, 2022.

[3] H. Huang, R. Liang, C. Lv, M. Lu, D. Gong, and S. Yin, Two-stage robust stochastic scheduling for energy recovery in coal mine integrated energy system, *Appl. Energy*, vol. 290, p. 116759, 2021.

[4] Y. Wang, H. Hu, X. Sun, Y. Zhang, and D. Gong, Unified operation optimization model of integrated coal mine energy systems and its solutions based on autonomous intelligence, *Appl. Energy*, vol. 328, p. 120106, 2022.

[5] Y. Wang, Y. Ma, F. Song, Y. Ma, C. Qi, F. Huang, J. Xing, and F. Zhang, Economic and efficient multi-objective operation optimization of integrated energy system considering electro-thermal demand response, *Energy*, vol. 205, p. 118022, 2020.

[6] T. Wu, S. Bu, X. Wei, G. Wang, and B. Zhou, Multitasking multi-objective operation optimization of integrated energy system considering biogas-solar-wind renewables, *Energy Convers. Manag.*, vol. 229, p. 113736, 2021.

[7] Y. Qiao, F. Hu, W. Xiong, Z. Guo, X. Zhou, and Y. Li, Multi-objective optimization of integrated energy system considering installation configuration, *Energy*, vol. 263, p. 125785, 2023.

[8] Y. Dong, H. Zhang, P. Ma, C. Wang, and X. Zhou, A hybrid robust-interval optimization approach for integrated energy systems planning under uncertainties, *Energy*, vol. 274, p. 127267, 2023.

[9] Y. Tian, T. Zhang, J. Xiao, X. Zhang, and Y. Jin, A coevolutionary framework for constrained multiobjective optimization problems, *IEEE Trans. Evol. Comput.*, vol. 25, no. 1, pp. 102–116, 2020.

[10] M. Ming, A. Trivedi, R. Wang, D. Srinivasan, and T. Zhang, A dual-population-based evolutionary algorithm for constrained multiobjective optimization, *IEEE Trans. Evol. Comput.*, vol. 25, no. 4, pp. 739–753, 2021.

[11] M. Ming, R. Wang, H. Ishibuchi, and T. Zhang, A novel dual-stage dual-population evolutionary algorithm for constrained multiobjective optimization, *IEEE Trans. Evol. Comput.*, vol. 26, no. 5, pp. 1129–1143, 2021.

[12] H. Ma, H. Wei, Y. Tian, R. Cheng, and X. Zhang, A multi-stage evolutionary algorithm for multi-objective optimization with complex constraints, *Inf. Sci.*, vol. 560, pp. 68–91, 2021.

[13] Z. Fan, W. Li, X. Cai, H. Li, C. Wei, Q. Zhang, K. Deb, and E. Goodman, Push and pull search for solving constrained multi-objective optimization problems, *Swarm Evol.*

Comput., vol. 44, pp. 665–679, 2019.

[14] A. Gupta, Y. S. Ong, and L. Feng, Multifactorial evolution: Toward evolutionary multitasking, *IEEE Trans. Evol. Comput*., vol. 20, no. 3, pp. 343–357, 2015.

[15] L. Feng, Y. Huang, L. Zhou, J. Zhong, A. Gupta, K. Tang, and K. C. Tan, Explicit evolutionary multitasking for combinatorial optimization: A case study on capacitated vehicle routing problem, *IEEE Trans. Cybern*., vol. 51, no. 6, pp. 3143–3156, 2020.

[16] P. T. H. Hanh, P. D. Thanh, and H. T. T. Binh, Evolutionary algorithm and multifactorial evolutionary algorithm on clustered shortest-path tree problem, *Inf. Sci*., vol. 553, pp. 280–304, 2021.

[17] K. Chen, B. Xue, M. Zhang, and F. Zhou, Evolutionary multitasking for feature selection in high-dimensional classification via particle swarm optimization, *IEEE Trans. Evol. Comput*., vol. 26, no. 3, pp. 446–460, 2021.

[18] K. Qiao, K. Yu, B. Qu, J. Liang, H. Song, and C. Yue, An evolutionary multitasking optimization framework for constrained multiobjective optimization problems, *IEEE Trans. Evol. Comput*., vol. 26, no. 2, pp. 263–277, 2022.

[19] K. Qiao, K. Yu, B. Qu, J. Liang, H. Song, C. Yue, H. Lin, and K. C. Tan, Dynamic auxiliary task-based evolutionary multitasking for constrained multiobjective optimization, *IEEE Trans. Evol. Comput*., vol. 27, no. 3, pp. 642–656, 2022.

[20] F. Ming, W. Gong, L. Wang, and L. Gao, Constrained multi-objective optimization via multitasking and knowledge transfer, *IEEE Trans. Evol. Comput*., doi: 10.1109/TEVC.2022.3230822.

[21] G. Wu, R. Mallipeddi, P. N. Suganthan, R. Wang, and H. Chen, Differential evolution with multi-population based ensemble of mutation strategies, *Inf. Sci*., vol. 329, pp. 329–345, 2016.

[22] R. Storn and K. Price, Differential evolution—A simple and efficient heuristic for global optimization over continuous spaces, *J. Glob. Optim*., vol. 11, no. 4, pp. 341–359, 1997.

[23] G. G. Wang, D. Gao, and W. Pedrycz, Solving multiobjective fuzzy job-shop scheduling problem by a hybrid adaptive differential evolution algorithm, *IEEE Trans. Ind. Inform*., vol. 18, no. 12, pp. 8519–8528, 2022.

[24] Z. J. Wang, Y. R. Zhou, and J. Zhang, Adaptive estimation distribution distributed differential evolution for multimodal optimization problems, *IEEE Trans. Cybern*., vol. 52, no. 7, pp. 6059–6070, 2020.

[25] Y. Wang, J. P. Li, X. Xue, and B. C. Wang, Utilizing the correlation between constraints and objective function for constrained evolutionary optimization, *IEEE Trans. Evol. Comput*., vol. 24, no. 1, pp. 29–43, 2019.

[26] E. Jiang, L. Wang, and J. Wang, Decomposition-based multi-objective optimization for energy-aware distributed hybrid flow shop scheduling with multiprocessor tasks, *Tsinghua Science and Technology*, vol. 26, no. 5, pp. 646–663, 2021.

[27] H. Zhang, J. Xie, J. Ge, J. Shi, and Z. Zhang, Hybrid particle swarm optimization algorithm based on entropy theory for solving DAR scheduling problem, *Tsinghua Science and Technology*, vol. 24, no. 3, pp. 282–290, 2019.

[28] K. Deb, An efficient constraint handling method for genetic algorithms, *Comput. Methods Appl. Mech. Eng*., vol. 186, nos. 2–4, pp. 311–338, 2000.

[29] T. Takahama and S. Sakai, Efficient constrained optimization by the ε constrained adaptive differential evolution, in *Proc. IEEE Congress on Evolutionary Computation*, Barcelona, Spain, 2010, pp. 1–8.

[30] Y. Chen, R. Wang, M. Ming, S. Cheng, Y. Bao, W. Zhang, and C. Zhang, Constraint multi-objective optimal design of hybrid renewable energy system considering load characteristics, *Complex Intell. Syst*., vol. 8, no. 2, pp. 803–817, 2022.

[31] Z. Hu, Z. Li, C. Dai, X. Xu, Z. Xiong, and Q. Su, Multiobjective grey prediction evolution algorithm for environmental/economic dispatch problem, *IEEE Access*, vol. 8, pp. 84162–84176, 2020.

[32] K. Deb, A. Pratap, S. Agarwal, and T. Meyarivan, A fast and elitist multiobjective genetic algorithm: NSGA-II, *IEEE Trans. Evol. Comput*., vol. 6, no. 2, pp. 182–197, 2002.

[33] H. Jain and K. Deb, An evolutionary many-objective optimization algorithm using reference-point based nondominated sorting approach, part II: Handling constraints and extending to an adaptive approach, *IEEE Trans. Evol. Comput*., vol. 18, no. 4, pp. 602–622, 2013.

[34] Y. Tian, R. Cheng, X. Zhang, F. Cheng, and Y. Jin, An indicator-based multiobjective evolutionary algorithm with reference point adaptation for better versatility, *IEEE Trans. Evol. Comput*., vol. 22, no. 4, pp. 609–622, 2017.

[35] Y. Tian, R. Cheng, X. Zhang, and Y. Jin, PlatEMO: A MATLAB platform for evolutionary multi-objective optimization[educational forum, *IEEE Comput. Intell. Mag*., vol. 12, no. 4, pp. 73–87, 2017.

[36] W. Fan, Z. Tan, F. Li, A. Zhang, L. Ju, Y. Wang, and G. De, A two-stage optimal scheduling model of integrated energy system based on CVaR theory implementing integrated demand response, *Energy*, vol. 263, p. 125783, 2023.

[37] L. Ma, M. Huang, S. Yang, R. Wang, and X. Wang, An adaptive localized decision variable analysis approach to large-scale multiobjective and many-objective optimization, *IEEE Trans. Cybern*., vol. 52, no. 7, pp. 6684–6696, 2021.

[38] W. Zhang, W. Hou, C. Li, W. Yang, and M. Gen, Multidirection update-based multiobjective particle swarm optimization for mixed no-idle flow-shop scheduling problem, *Complex System Modeling and Simulation*, vol. 1, no. 3, pp. 176–197, 2021.

[39] Z. Cui, L. Zhao, Y. Zeng, Y. Ren, W. Zhang, and X. Z. Gao, Novel PIO algorithm with multiple selection strategies for many-objective optimization problems, *Complex System Modeling and Simulation*, vol. 1, no. 4, pp. 291–307, 2021.

[40] X. Xu, Z. Hu, Q. Su, Z. Xiong, and M. Liu, Multi-objective learning backtracking search algorithm for economic emission dispatch problem, *Soft Comput.*, vol. 25, no. 3, pp. 2433–2452, 2021.

Canyun Dai received the MS degree from Yangtze University, Jingzhou, China in 2021. She is currently pursuing the PhD degree at School of Information and Control Engineering, China University of Mining and Technology, China. Her research interests include integrated energy systems and intelligent optimization.

Xiaoyan Sun received the PhD degree in control theory and control engineering from China University of Mining and Technology, Xuzhou, China in 2009. She is a professor at School of Information and Control Engineering, China University of Mining and Technology, China. Her research interests cover evolutionary computation and machine learning.

Hejuan Hu received the MS degree from North China University of Water Resources and Electric Power, Zhengzhou, China in 2017. She is currently pursuing the PhD degree at School of Information and Control Engineering, China University of Mining and Technology, China. Her research interests include integrated energy systems modeling and optimization.

Yong Zhang received the PhD degree in control theory and control engineering from China University of Mining and Technology, Xuzhou, China in 2009. He is a professor at School of Information and Control Engineering, China University of Mining and Technology, China. His research interests cover swarm intelligence and machine learning.

Dunwei Gong received the PhD degree in control theory and control engineering from China University of Mining and Technology, Xuzhou, China in 1999. He is a professor at School of Information Science and Technology, Qingdao University of Science and Technology, China. His current research interests include computation intelligence in multi-/many-objective optimization, dynamic and uncertain optimization, as well as applications in software engineering, integrated energy systems, scheduling, and healthcare.